Convective exchange between the nose and the atmosphere

F. R. HASELTON AND P. G. N. SPERANDIO
Cardiovascular-Pulmonary Division, Department of Medicine, Hospital of the University of Pennsylvania, Philadelphia, Pennsylvania 19104

HASELTON, F. R., AND P. G. N. SPERANDIO. *Convective exchange between the nose and the atmosphere.* J. Appl. Physiol. 64(6): 2575–2581, 1988.—It is generally accepted that there is little rebreathing of gas exhaled through the nose. A detailed physical model system has been used to quantify and identify the mechanisms responsible for this phenomenon. By the use of a cast of the upper respiratory tract and oscillating flows with a Reynolds number of 500 and nondimensional frequency of 1.6, corresponding to quiet tidal breathing through the nose, dye dilution measurements indicated an efficiency of tidal exchange of 0.95. Flow visualization studies performed to trace the expiratory flow, as well as the streamlines during steady inspiratory flow, support the hypothesis that the high efficiency of exchange is due to radical differences in the velocity fields between inspiratory and expiratory phases of this oscillatory flow. These findings confirm that convective gas exchange between the nose and the atmosphere is highly efficient; however, the underlying mechanism responsible for this exchange also maximizes the exposure of the respiratory system to aerosols contained in the ambient atmosphere.

gas exchange; aerosols; flow visualization

MUCH ATTENTION has been given to the exchange of gases along the airways and across the alveolar-capillary membrane, but surprisingly little has been said about gas exchange between the nose and the ambient atmosphere. There are at least two reasons why this process is of interest. In the case of gas exchange, a volume of exhaled gas that is reinhaled would affect the composition of gases in the upper airways and ultimately the gas concentrations at the alveolar-capillary membrane. Although it is generally assumed that each inhaled breath contains entirely fresh gas and no exhaled gas, this has never been measured. Second, in the case of breathing an atmosphere containing aerosols, the exchange process between the nose and the atmosphere determines the number of aerosol particles inhaled into the respiratory system. This factor may be important for making realistic estimates of respiratory aerosol exposure due to environmental aerosols such as those occurring in passive smoking.

Convection and diffusion both influence gas exchange everywhere along the respiratory tract. However, the introduction of fresh gas into the respiratory system via the nose has two important features that are quite the opposite from the exchange conditions that occur in the alveolar region at the bottom of the lung. First, the velocity of the gases at the nose is much greater than in the alveolar region, and second, the interfacial area between the exhaled gas outside the nose and fresh gas about to be inhaled at the nose is much less than in the total interfacial area occurring in the alveolar region. In the same way that low velocities and the large interfacial area lead to the conclusion that diffusional exchange dominates in the bottom of the lung, it can be argued that the high velocities and the small interfacial area lead to the conclusion that convection dominates in the exchange process occurring between the nose and the atmosphere.

The experiments described in this study examine the convective exchange process occurring between the nose and the atmosphere during quiet nasal breathing. For the first time, the efficiency of the exchange was measured quantitatively. Flow visualizations for expiratory and inspiratory flow were also carried out to further characterize the convective flow patterns. A convective exchange mechanism is suggested that accounts for the efficiency measurements and the flow patterns observed.

METHODS

Physical model studies were used to explore the convective features of exchange between the nose and the atmosphere. First, we measured the volume exchanged between the nose and the atmosphere in a purely convective system, and second, using a flow visualization technique, we directly observed the flow patterns during both expiration and inspiration.

A key feature of our model system is that we studied the motion of a liquid rather than the motion of a gas. This approach allowed us to separate the effects of convection from those of diffusion. Convective effects predominate in a liquid system, since the coefficient of diffusion of a liquid tracer in the surrounding liquid is nearly 10,000 times less than the coefficient of diffusion of a tracer gas in the surrounding gas. The use of a liquid system also permitted the use of visualization techniques that are more difficult to apply in a gas system.

The disadvantage of a liquid model system is that only under restricted experimental conditions can the model results be directly applied to the corresponding gas system. We used the conditions of geometric and dynamic similarity to establish correspondence between observations made in our model system and predictions of gas behavior in the respiratory system. Geometric similarity

states that the model must have the same geometric shape with respect to the real system, and dynamic similarity is based on the idea that if the same balance of forces in the real and model systems can be achieved, then the same phenomena will be observed. The balance of important forces acting in the system is measured by the magnitude of selected dimensionless groups. When the values of these dimensionless groups are matched between the model and real systems, then the observations made in a model system may be inferred to occur in the real system (2).

In pursuing this approach, we were fortunate to have the use of a cast of the upper respiratory tract (URT) from the trachea to the nares (3). Because this model in these studies is a replica of the same size as the actual human anatomy, geometric similarity was automatically achieved. Dynamic similarity in our model system was achieved by matching the Reynolds number ($\mathrm{Re} = 2Vf/r\pi\nu$) and the Womersley frequency parameter ($\alpha = r\sqrt{(2\pi f/\nu)}$) between the two systems. In these expressions V is the tidal volume (cm^3), f is the oscillatory frequency (Hz), r is the radius of the nare, and ν is the kinematic viscosity (cm^2/s). Re represents the ratio of inertial to viscous forces and in the URT model was defined for half the tidal volume flowing through one nare; α represents the ratio of accelerative to viscous forces. To achieve dynamic similarity between air breathing through the nose and liquid breathing in the model, both Re and α in the nose and the nose model must have the same value. This required that f/ν be in the same ratio. Because the ratio of air to water viscosity is ~15, the breathing frequency in the model was lowered by a factor of 15.

Convective exchange methods. The system for measuring the convective exchange efficiency consisted of a tank, a Harvard ventilator pump, and the URT model. Oscillating flows within the model system were driven by the Harvard pump connected to the tracheal end of the model. The model was immersed in a glass tank filled with tap water containing sodium fluorescein dye (~1 μg/ml). The water in the tank represents the ambient atmosphere in this model system. The URT model, tubing, and pump contained undyed water. The length of the tubing was chosen so that the volume of the tubing was greater than twice any tidal volume used to eliminate the loss of dye inside the pump. Because preliminary experiments suggested that the system was sensitive to very small density differences caused by temperature variations, the system was maintained in a temperature-controlled room and allowed to equilibrate overnight before an experiment was performed.

The exchange of liquid between the oscillating volume and the surrounding water was measured using a dye dilution technique. The model, pump, and connecting tubing were filled with undyed water from a temperature-equilibrated reservoir and sealed by placing a plug into each nare. The model was then immersed in the tank and the plugs were removed. After the tank was allowed to settle for a few minutes, the pump was started and allowed to turn for one cycle, expiration followed by inspiration. The plugs were reinserted into the model, the model was removed from the tank, and the contents of the model were collected in a beaker. The volume of the drainage and washings from the model was recorded using volumetric flasks. Dye concentration of the model drainage and washings and of a sample for the tank water taken before the start of the experiment was measured with a fluorometer and used to calculate the volume of fluid transferred from the tank to the interior of the model. This formula was derived from a simple conservation of mass within this system and is given by

$$\text{volume exchanged} = \frac{\text{model concn} \cdot \text{vol of washings from model}}{\text{tank concn}}$$

The tidal volume was measured in a similar experiment where the pump was stopped in the middle of the cycle between expiration and inspiration. The model plugs were inserted, and the tank water was thoroughly mixed. The model was unsealed, and the experiment was then continued as above. This procedure was used to measure tidal volume and minimize any systematic experimental error due to dye leakage when the model was sealed. The exchange efficiency was then calculated as

$$\text{exchange efficiency} = \frac{\text{vol exchanged over a flow cycle}}{\text{tidal vol}}$$

Measurements were made using this model system at Re and α values found during quiet nasal breathing of gases (Re = 500, α = 1.6). To determine the effect of changing tidal volumes on the efficiency of the exchange, the experiments using the URT model were repeated for three different Re values ranging from ~100 to 800; α was constant at 1.6.

In measuring the fluorescence of the samples, the same cuvette was used for each measurement within one experiment. Six sample readings were taken for each experiment, and the average of these values was used.

Since the actual size of the model limited the range of Re and α values investigated, the same experiments were also performed using the same experimental design and a straight cylindrical tube rather than the URT model. The straight tubes were used to investigate the effect of Re over a much broader range. The radius of the rigid tubing used in these experiments varied between 1 and 0.1 cm. In some of these experiments, water-glycerine mixtures and an infusion pump were used to make measurements at the lowest Re value. In these experiments Re and α varied together (range 0.004–700 and 0.01–4.2, respectively).

Flow visualization methods. A flow visualization study was performed to better understand the flow fields during the oscillatory flow. These methods were used to visualize the flow during both the expiratory and inspiratory phases of nose breathing. To visualize the flow during expiration, a liquid dye method using the hollow cast URT model described above was developed (see Fig. 1*A*). This method of visualization has been previously described (4, 5). The model, the connecting tubing, and the pump were filled with water containing white opaque beads that were neutrally buoyant. Photographs of the

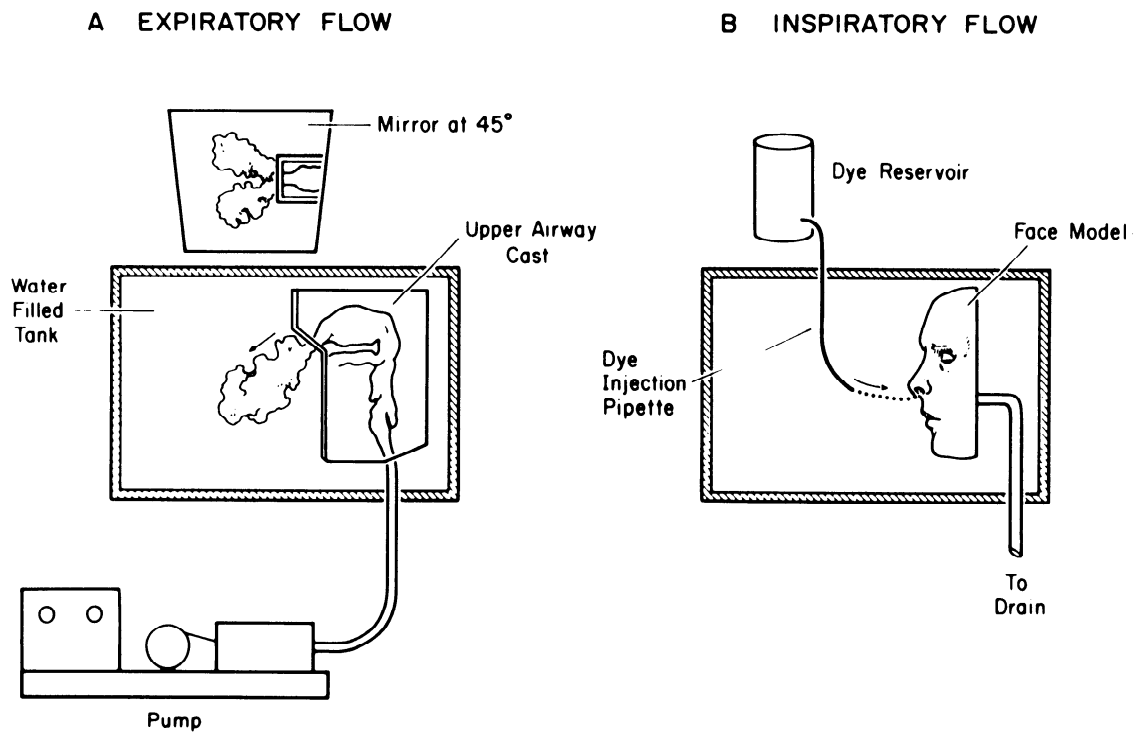

FIG. 1. Schematic design of flow visualization methods used for expiratory flow (A) and inspiratory flow (B).

motion of the exhaled volume were taken as fluid was pumped from the model at a Re corresponding to quiet nose breathing.

Visualizing the flow during the inspiratory phase required a slightly different method. During inspiration the geometry internal to the nasal cavity does not affect the external flow field; however, the shape of the face may be important. Therefore a full-size mask of the face was used to visualize the inspiratory phase of the flow. The mask was submerged in the tank system and water was drained from the tank through the nose of the facemask via Tygon tubing connected to the back of the mask (see Fig. 1B). This visualization method was used to define the streamlines or fluid particle paths found in a steady flow into the nose at a nare Re ($\dot{Q}/2\pi r\nu$) of 500, where $\dot{Q}$ is the total flow rate out of the tank (cm^3/s). To trace the motion of the fluid streamlines, a solution of sodium fluorescein was injected at a controlled rate from a pipette in the vicinity of the region to be visualized. The dye formed a streamline from the pipette exit to the entrance of the nose. By moving the pipette to various positions and making multiple exposures, a pattern of the flow was traced out. These photographs were used to crudely estimate the relative strength of the velocity field as the dye stream approached the entrance of the nose, by assuming that the width of the dye at any given position was inversely proportional to the local velocity that the streamline experienced (1).

Similar visualizations were also performed in straight-tube geometry. The above procedures were employed with a straight tube with internal diameter of 0.8 cm and length of 5 cm in place of the URT model and the face model, respectively. Re and α during the expiration flow were 500 and 1.6, respectively. During the steady inspiration visualization experiments Re was 500.

RESULTS

Figure 2 is a plot of the convective exchange efficiency (volume exchanged/tidal volume) as a function of Re. The convective exchange efficiencies were >0.95 and were independent of Re over a range from ~100 to 800 at α of 1.6.

In the straight tube the exchange is the same as that found in the more complex nasal geometry at the same Re and α values. Figure 3 is a plot of the same experimental design carried out using a straight-tube geometry over a much wider range of the Re and α. Exchange efficiency was ~0.95 until Re and α decreased to <10 and <1.3, respectively. However, over a wide range, the exchange efficiency is found to vary little, even to values as low as a Re of 10 and an α of 1.3. Below these values

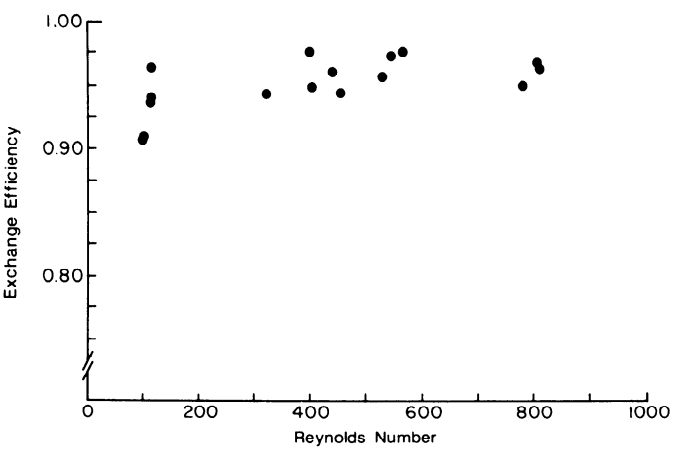

FIG. 2. Exchange efficiency as a function of Reynolds number for nose breathing. Reynolds number ranges from 100 to 800 and frequency parameter (α) is constant at 1.6.

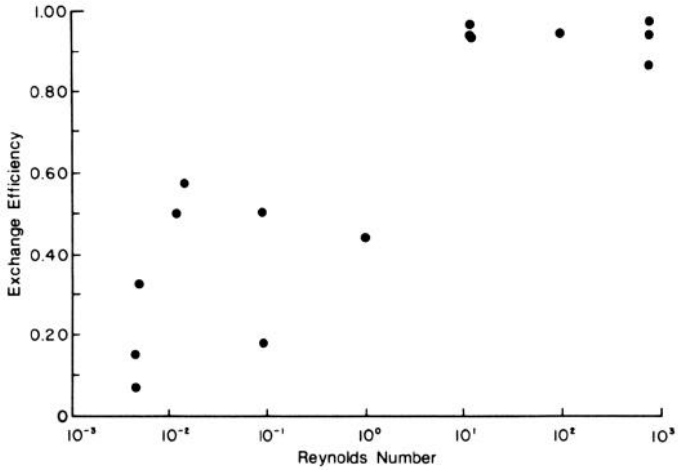

FIG. 3. Exchange efficiency as a function of Reynolds number over a wide range of Reynolds numbers for oscillating flow between a straight tube and a reservoir.

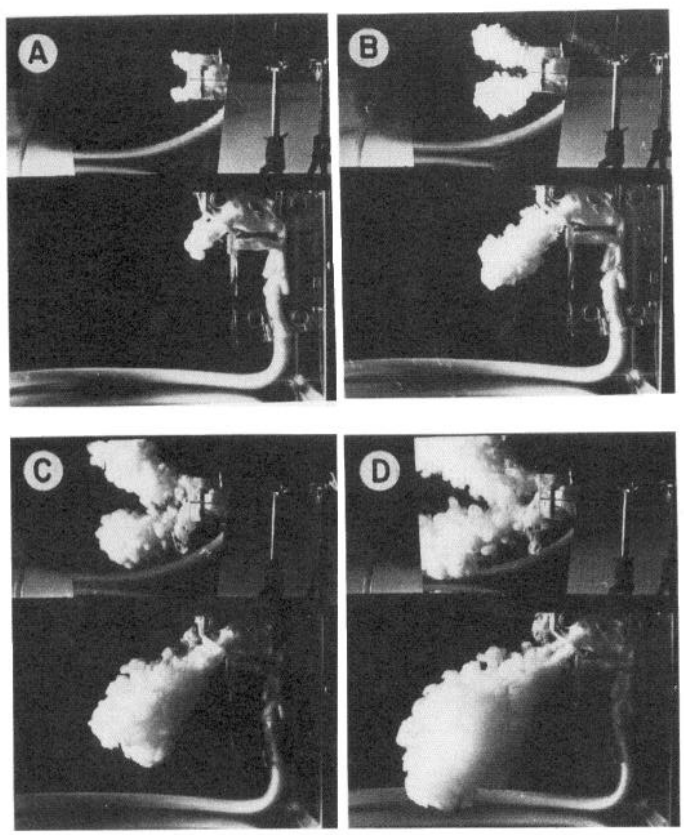

FIG. 4. Four photographs of visualization of flow during expiration from nose. Upper respiratory tract model is in *bottom right* in each frame and is best seen in *A*. In each frame there is a mirror suspended at 45° above model. Frames show flow at 1/16 of cycle (*A*), 1/8 (*B*), 3/16 (*C*), and 1/4 (*D*).

the exchange efficiency decreased, indicating the rising importance of fluid viscosity.

Visualization of the expiratory flow is shown in the sequence of photographs in Fig. 4, which shows the shape of the expired tidal volume bolus exhaled through the nares at four times during the expiratory cycle. At the top of these photographs is the overhead view seen in a mirror placed at 45° to the vertical plane (see Fig. 1*A*). These photographs suggest that during the expiratory phase the flow field is confined to a narrow high-speed region.

The inspiratory profiles during steady flow into a nose model are shown in Fig. 5, which shows a frontal, a medial, and a superior view. The flow in these experiments is more uniformly distributed so that flow toward the nose has almost the same magnitude from all directions.

DISCUSSION

These model results imply that the gas inspired during nose breathing consists almost entirely of fresh gas. In these experiments, direct measurements of the exchange of liquid between the upper respiratory tract model and the surrounding liquid bath had an exchange efficiency of >95% under all conditions. These experiments were carefully designed, including making measurements using a cast of the upper respiratory tract, so that the results could be directly interpreted with respect to the exchange of gases between the nose and the atmosphere.

What convective mechanisms can account for the efficient exchange of gases during their oscillatory flow in

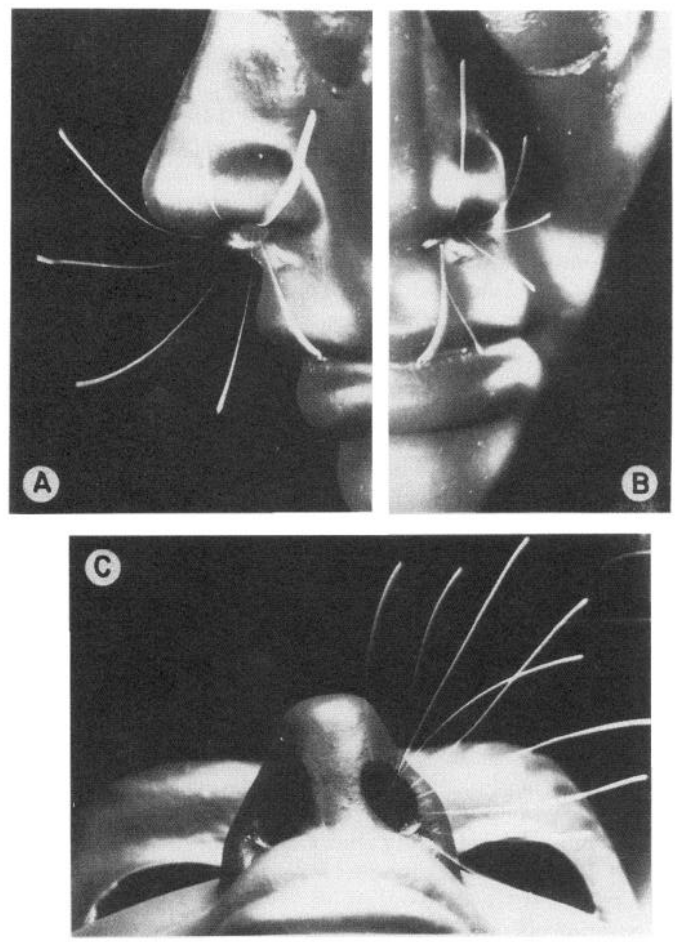

FIG. 5. Visualization of streamlines found during steady inspiratory flow at a Reynolds number of 500. Three views obtained during separate experiments are shown. *A*: side view with dye probe positioned in 7 locations near midsagittal plane. *B*: front view with dye probe positioned in 5 locations in a coronal plane just in front of face. *C*: front view with dye probe positioned in 8 locations in horizontal plane just below nose.

this region? One possible explanation is turbulent mixing of the exhaled gases with the ambient atmosphere. This postulate is summarized in the comment of Rouse (8), "Even the act of breathing depends upon turbulence, for without the violent mixing which accompanies exhalation no fresh air could be inhaled thereafter unless one moved to a new location." According to this mechanism, the exhaled volume has become sufficiently diluted so that no substantial portion is rebreathed. This possible explanation cannot be rejected out of hand, since there is no doubt that near the exit of the nose the flow of gas is highly mixed.

However, another possible mechanism that may account for the system's apparent efficiency, the nonreversing flow fields found during this oscillatory flow, is hinted at in a footnote by Batchelor (1), "A match can be extinguished by blowing, but not by sucking!" He makes this comment to emphasize that the high velocity found during exhalation is possible because the majority of the gas is concentrated in a narrow stream but during inhalation, the gas inspired comes from all directions and hence with a lower more uniform velocity.

The photographs of the flow visualization experiments in Figs. 4 and 5 show that the flow fields are radically different when expiratory flow is compared with inspiratory flow. The expiratory flow is highly mixed and most probably turbulent in character at the Re of 500 found during normal breathing. Although no direct measurements were made that would imply turbulence, it is known that a turbulent jet produces a conical turbulent region with a constant total angle of between 25 and 30° (6). Measurements made on the photographs shown in Fig. 4 have a constant total angle of ~23°, which is consistent with other turbulent jet measurements.

Inspiratory flow is quite different. The photographs of Fig. 5 show that this flow is certainly not turbulent, i.e., it is laminar, and contrary to the narrow cone found during expiration, the flow approaches the entrance of the nose from all possible directions as previously proposed by Swift and Proctor (9). The best description of the complete flow field found in the steady-flow experiments is that of flow into a three-dimensional sink. The characteristics of idealized inviscid flow into a sink in a plane are that the radial velocity components are the only nonzero components of flow, are independent of the angular coordinate, and have magnitudes that vary inversely as the square of the distance from the sink. These characteristics are well illustrated in the photographs of Fig. 5. The streamlines are predominantly directed toward the nare, as they should be if all other velocity components other than radial are zero. The independence of angular coordinate can be implied by comparing the width of the dye traces when the dye probe is placed in different positions. Because the flow rate of dyed fluid out of the flow probe is constant, the width of the white trace is inversely proportional to the local velocity. For incompressible steady or slowly time-varying flow, the dye filaments are stream tubes whose width is inversely proportional to local fluid velocity (1). Within the resolution of these methods, the width of the traces from all directions at a given distance is approximately the same. The fact that the dye trace decreases in width as the dye moves closer to the nare shows that the local velocity is increasing as a function of radial position. The correspondence between the visualization experiment and the idealized sink flow is not exact, and minor differences are most probably due to the stagnant boundary layer near the face and slight density differences between the dyed fluid and the surrounding undyed fluid. It is somewhat surprising that even when the dye probe was placed very near the face, a significant flow toward the nose was still detectable (see Fig. 5*A*, trace at 1:00).

Based on the major differences observed in the flow visualization experiments during expiration and inspiration, we propose that a convective exchange mechanism can account for the high exchange efficiency observed in the model system. Figure 6 is an idealized schematic showing the position of the expired gas immediately after expiration and the position of the inspired gas immediately before inspiration. The position of the expiratory gas is based on the expiratory flow visualization, which showed a narrow 23° jet issuing from the nose. Similarly the position of the soon to be inhaled gas is based on the inspiratory flow visualization, which showed that fluid enters the nares from all directions.

The purpose of this diagram is to illustrate the small volume of intersection between these two regions. This intersectional volume is the volume of exhaled gas that will be rebreathed during the next inspiration. The volume of the soon to be inhaled gas that is not within this intersectional region is the source of fresh gas for the next breath.

Not only does this diagram match the visualization results in shape, but in addition, a calculation of the intersectional volume of a 23° angle cone with a 500-cm^3 hemisphere is ~10 cm^3. This leads to a calculated convective exchange efficiency of 0.98, which is very close to the 0.95 value obtained in the dye dilution studies.

The visualization results provide strong evidence for this being the best explanation of the high exchange efficiency observed in the dye exchange experiments. Several alternative explanations are turbulent mixing as suggested by Rouse (8), diffusional exchange, and cur-

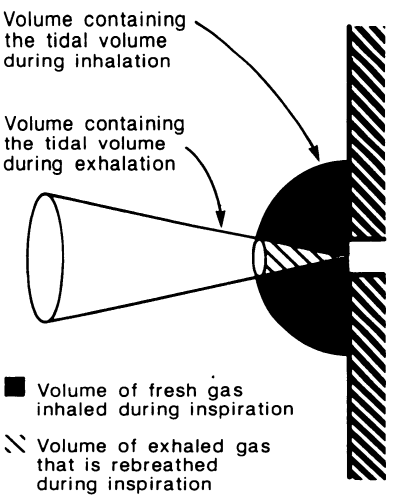

FIG. 6. Schematic diagram showing operation of hypothetical convective exchange mechanism.

rents in the reservoir. Because the same experimental apparatus was used in both the dye exchange and the flow visualization experiments, the behavior of the visualized flow should have closely matched the flow occurring in the dye exchange experiments. Any turbulent mixing that does occur is evidently confined within the narrow 23° conical volume extending far out in front of the nose as shown in Fig. 4. In addition, Fig. 3 provides further evidence that the turbulent character of the expiratory flow is not the major explanation. As Fig. 4 shows, when exchange efficiency was measured for Re as low as 10, which more closely represents conditions found in a laminar jet (7), the exchange efficiency was still 0.90–0.95. The second alternative explanation, mixing by diffusing, is minimized by the experimental design. Evidence for this is seen in the narrow streams of Fig. 5. If diffusion were significant compared with convection in this liquid system, these streams would have a much broader shape and less clearly defined edges. The third possible explanation, i.e., reservoir currents, can also be dismissed based on the photographic results. Significant currents would be readily evident in the shape of the dye streams during the inspiratory phase and in the distribution of the exhaled volume.

In the original design of the exchange experiments, the geometry of the upper respiratory tract was thought to be an important factor, and this was the reason a cast of the upper airways was used. To investigate the importance of this geometry, a straight tube was substituted for the complex upper airway model. The straight tube also allowed an investigation of the theoretical prediction that in the limit of zero Re number and α, the flow fields would approach reversibility, and the exchange would be zero (5). Because straight tubes were readily obtainable in a variety of diameters, whereas the cast is of a fixed size, this greatly simplified a more detailed exploration of dependence of the efficiency of exchange on the Re and α parameters. As Fig. 3 shows, at a Re between 10 and 1,000, the efficiency of exchange remained almost the same for the straight tube. By the use of the straight-tube geometry, measurements were made at Re as low as 0.04 (with $\alpha = 0.01$). These measurements show a decrease in the exchange efficiency as Re and α decrease. There was also a much greater scatter in these measurements, but the trend is clearly that exchange, in agreement with theoretical expectations, is approaching zero.

The experimental model is geometrically and dynamically similar to flows found in quiet nose breathing. To the extent that this is true, the results accurately represent results that would have been obtained in more complex experiments using the real nose. The model system was used, since this greatly simplified the experimental procedure and allowed us to isolate convective effects from diffusional effects that would complicate measurements made using gases. In designing these experiments, we expected diffusional effects to be minimal. This was based, in part, on the large value of the Peclet number, which represents the relative contribution of convection to diffusion in a flowing gas (Ud/D) and is ~600 at the nose during normal breathing. The results of the model experiments indicate that exchange efficiency is high in the absence of significant diffusional effects, since the beads and the dye have a coefficient of diffusion at least five orders of magnitude less than coefficients of diffusion of gases. The presence of significant diffusion could raise the exchange efficiency, lower the efficiency, or have no effect. Raising or having no effect on the efficiency would not significantly change the efficiency of gas exchange, since 0.95 efficiency is already very high. If diffusion does significantly degrade the efficiency, it would have to transfer exhaled gas into the volume of the next inspiration. Although simultaneous convection and diffusion are complex, a simplified picture can give some qualitative indication of the importance of diffusion to the process. Since, based on the inspiratory flow field, the shape of the next volume is approximately a hemisphere with a short radius, the area of exchange between the expiratory and inspiratory volumes must be within this radius, i.e., closest to the nose. This area is the boundary of the intersecting volumes shown in Fig. 6. This region has the smallest interfacial area and the highest linear velocity, both of which would minimize the diffusional transfer. So while some contribution of diffusion to the exchange cannot be completely ruled out, significant diffusional exchange does not appear to be likely.

Two potentially important features of nose breathing that were not investigated in these experiments are the contribution of currents in the atmosphere and the effect of temperature and humidity differences between exhaled gases and the ambient atmosphere. With respect to air currents, one would expect the exchange ratio in the presence of significant air currents to be very close to 1, since exhaled gas would be rapidly transported away from the nose. Our results are most important in evaluating mechanisms operating during quiet nose breathing in an environment with small air currents, such as occurs during sleep in an enclosed room. The effects of differences in temperature and humidification between the exhaled gases and the ambient air will produce small density differences. These would be expected to have a minimal effect on exchange, since based on the visualization results, the exhaled volume does not have a significant intersectional volume with the inspired volume.

These results may have important implications for estimating the exposure of the respiratory system to environmental aerosols. Because the convective exchange efficiency is high, each inspiratory breath contains new aerosol particles, i.e., no exhaled aerosols are reinhaled. Evidently, breathing in an aerosol-laden environment will result in maximal inhalation of aerosol particles and hence maximal exposure of the respiratory system to these particles.

The authors thank D. Barrett and B. Lefferts for their expert assistance in preparing the manuscript.

The model of the upper respiratory tract was constructed by Dr. L. M. Hanna (see Ref. 3). Through the generosity of Dr. Hanna and Dr. P. W. Scherer, this model was made available for these exchange studies.

Received 27 July 1987; accepted in final form 4 January 1988.

REFERENCES

1. BATCHELOR, G. K. *An Introduction to Fluid Dynamics.* Cambridge, UK: Cambridge Univ. Press, 1967, p. 88.
2. BUCKINGHAM, E. On physically similar systems: illustrations of the use of dimensional equations. *Physiol. Rev.* 4: 345–376, 1914.
3. HANNA, L. M., AND P. W. SCHERER. Measurement of local mass transfer coefficients in a cast model of the human upper respiratory tract. *Trans. ASME J. Biomech. Eng.* 108: 12–18, 1986.
4. HASELTON, F. R., AND P. W. SCHERER. Bronchial bifurcations and respiratory mass transport. *Science Wash. DC* 208: 69–71, 1980.
5. HASELTON, F. R., AND P. W. SCHERER. Flow visualization of steady streaming in oscillatory flow through a bifurcating tube. *J. Fluid Mech.* 123: 315–333, 1982.
6. LANDAU, L. D., AND E. M. LIFSHITZ. *Fluid Mechanics.* New York: Pergamon, 1959, p. 132–133.
7. PAI, S. I. *Fluid Dynamics of Jets.* New York: Van Nostrand, 1954.
8. ROUSE, H. *Elementary Mechanics of Fluids.* New York: Dover, 1978, p. 2.
9. SWIFT, D. L., AND D. F. PROCTOR. Access of air to the respiratory tract. In: *Respiratory Defense Mechanisms,* edited by J. D. Brain, D. F. Proctor, and L. M. Reid. New York: Dekker, 1977, vol. 5, pt. 1, p. 63–93. (Lung Biol. Health Dis. Ser.)